Lab on a Chip

PAPER

View Article Online
View Journal | View Issue

Cite this: *Lab Chip*, 2025, **25**, 4422

Hydrogel beads for enhanced nucleic acid analysis in complex fluid matrices†

Lokman Alpsoy, [ab] Stephan Tieu, [a] Sina Dehestanizad, [a] Thomas Brandstetter [a] and Jürgen Rühe *[ab]

We present a functionalized hydrogel bead platform designed to capture cell-free DNA (cfDNA), which is released from tumor cells into the bloodstream, and the use of this cfDNA as a biomarker for cancer detection. Hydrogel beads with covalently incorporated probes (HBP) are generated *via* photo-cross-linking in a two-phase microfluidic system. The precursor solutions from which the beads are generated are comprised of a photoreactive copolymer, magnetic nanoparticles, Cy3-labelled oligonucleotides serving as a barcode for bead identification, and a specific probe designed to bind the target DNA. From these solutions, droplets are generated in the microfluidic system and photocross-linked through C, H-insertion cross-linking (CHic). As a demonstration case, the hydrogel beads are used to detect a mutation (c.1633G>A) in MCF-7 cells, which is known to promote breast cancer progression by activating oncogenic signalling pathways. The HBPs were successfully employed to detect a fluorescently labelled mutation sequence (92 bp) in phosphate-buffered saline (PBS), serum, and whole blood using a fluorescent reader, followed by amplification through polymerase chain reaction (PCR). The sensitivity of the cfDNA detection method described here demonstrates a detection limit as low as 0.36 ng mL^{-1}, which is lower than any other detection limit in the literature so far. The sensitivity of the hydrogel bead platform can be further significantly increased. This is because beads containing the captured DNA can be subjected directly to PCR for the amplification of the target sequence, eliminating the need for any additional purification steps. The simplicity of production, modification, and functionalization of the hydrogel beads, coupled with their high sensitivity in detecting cfDNA, makes this platform a promising approach for diagnosing a range of diseases.

Received 7th May 2025,
Accepted 25th June 2025

DOI: 10.1039/d5lc00447k

rsc.li/loc

1. Introduction

Traditionally, cancer has been diagnosed and characterized using tissue biopsies, which require the removal of a tumor sample from the patient for detailed laboratory analysis. Accordingly, the development of liquid biopsy techniques for monitoring cancer progression and therapeutic response has become an emerging and rapidly growing area of research.[1] Liquid biopsies typically involve the extraction and analysis of biomolecules such as DNA, RNA, proteins, and extracellular vesicles from body fluids, including blood, urine, saliva, and cerebrospinal fluid.[2,3] Circulating free DNA (cfDNA), particularly the tumor-derived circulating tumor DNA (ctDNA) fraction, has become an increasingly valuable biomarker for cancer diagnosis and monitoring.[3,4] cfDNA is typically fragmented into small pieces with a size distribution of approximately 130–170 base pairs (bp), which corresponds to the length of DNA wrapped around nucleosomes and results from enzymatic cleavage by nucleases.[5] cfDNA is released into the bloodstream through a variety of mechanisms, including apoptosis, necrosis, and active cellular secretion.[2–4] The levels of ctDNA frequently correlate with the extent of the tumor growth and can serve as a predictor of response to targeted therapies and immunotherapies.[2,5] In addition, ctDNA provides insight into tumor heterogeneity and the emergence of therapy-resistant clones.[2]

Bead-based technologies play a crucial role in liquid biopsies for the collection of both circulating tumor cells (CTCs) and cfDNA.[6] The use of antibody-coated magnetic beads allows for the effective isolation of EpCAM-positive CTCs. The BEAMing (beads, emulsion, amplification, and magnetics) method provides a high sensitivity for the detection of rare genetic variants in cfDNA. Additionally, streptavidin-coated magnetic beads with biotin-conjugated probes facilitate the selective isolation of cfDNA fragments, increasing the versatility and significance of bead-based methods in cancer diagnostics.[4,6,7]

[a] *Department of Microsystems Engineering (IMTEK), Chemistry & Physics of Interfaces, University of Freiburg, 79110 Freiburg im Breisgau, Germany. E-mail: ruehe@imtek.de*
[b] *Freiburg Center for Interactive Materials and Bioinspired Technologies (FIT), University of Freiburg, 79110 Freiburg im Breisgau, Germany*

† Electronic supplementary information (ESI) available. See DOI: https://doi.org/10.1039/d5lc00447k

A major challenge in the application of ctDNA as a biomarker is the limited sensitivity of the analytical methods developed to date. ctDNA is typically present only at very low concentrations in biofluids, particularly in early-stage cancers, making it difficult to reliably detect small tumor loads. This limitation hinders to make full use of the potential of ctDNA-based liquid biopsies for early cancer screening and monitoring of minimal residual disease.[8,9] The use of commercial kits and magnetic beads enables the detection of cfDNA at a concentration of ng mL^{-1}, which is considerably sufficient for the levels commonly observed in advanced cancers.[10–13] The use of various cfDNA isolation kits has resulted in the recovery of cfDNA at concentrations ranging from 3 to 13 ng mL^{-1} in plasma.[14] However, a disadvantage of the current methods is that they require sample sizes between 0.5 and 10 mL, which may not be feasible in some cases.[13] In addition, the potential for false results and the current lack of standardization across test platforms and methodologies pose challenges for liquid biopsies.[5]

Hydrogel beads offer a promising solution to enhance the sensitivity of ctDNA and CTC detection. Their porous and three-dimensional (3D) structure provides a large surface area, significantly enhancing the binding capacity compared to solid (*i.e.*, non-swellable) beads and traditional two-dimensional (2D) chip surfaces. This much larger surface area enhances the efficiency of ctDNA capture, thereby improving the sensitivity of the detection platform.[15] In addition, hydrogel beads are relatively easy to fabricate and functionalize, making this platform highly attractive for various diagnostic applications. For functionalization of the hydrogel beads, capture molecules such as antibodies, probes or proteins can be immobilized on the beads using different strategies including affinity interactions, where biomolecules are attached to beads through specific binding events, such as biotin-streptavidin or antigen–antibody interactions. Alternatively, covalent conjugation using chemical or cross-linking strategies offers a more stable attachment, ensuring stronger and more durable interactions between probe and bead.[16] One particularly effective method for probe immobilization on hydrogel beads is the carbon–hydrogen insertion cross-linking (CHic) reaction.[17,18] To generate the beads, appropriate precursor solutions are subjected to two-phase flow so that small droplets of polymer solution are generated. Using a cross-flowing stream within a T-junction, monodisperse hydrogel beads can be fabricated efficiently. Additionally, the bead size can be tuned by adjusting the flow rate ratio between the carrier and dispersed phases.[17] During photochemical activation, the polymer becomes cross-linked by C, H insertion reactions, and water-swollen hydrogel beads are formed. In the course of this reaction, any other organic molecules present in the solution are covalently attached to the forming networks. This technique enables the generation of beads with stable and covalent attachment of DNA or RNA probes to the bead surface without compromising the structural integrity of the probes. The result is a robust platform that enhances both the capture efficiency and sensitivity in ctDNA detection.

Incorporating magnetic properties into hydrogel beads further enhances the platform's ease of use and performance. Using magnetic hydrogel beads simplifies the washing steps during ctDNA capture as they can be easily separated from the solution using magnetofection. This process facilitates the efficient recovery of ctDNA, minimizes sample loss, and reduces the risk of contamination.[19,20] Additionally, magnetic bead-based platforms are user-friendly, allowing for easy handling and rapid processing in both manual and automated workflows. This makes the platform particularly well-suited for high-throughput screening and diagnostic applications (Fig. 1).

The aim of this study is to develop and fabricate the HBP incorporating magnetic nanoparticles and DNA capture probes using microfluidic assembly and UV-cross-linking approach. To demonstrate the efficacy of this platform, hydrogel beads were employed to capture a Cy5-labeled mutation sequence (c.1633G>A) in MCF-7 cells in a variety of media, including phosphate-buffered saline (PBS), serum, and whole blood. This mutation in MCF-7 promotes breast cancer progression by activating the PI3K/AKT/mTOR oncogenic signalling pathways. Understanding the role of this mutation is essential for personalizing treatment strategies to improve patient survival rates in breast cancer therapy. We investigated the extent to which the produced beads can be used directly in PCR processes, thereby eliminating the need for traditional DNA isolation. We also studied the capture of the same MCF-7 sequence from natural, unlabelled DNA samples.

2. Materials and methods

Production of hydrogel beads by the microfluidic system

The copolymer P(DMAA-*co*-6% MABP-*co*-2.5% SSNa) was synthesized according to Rendl *et al.*[21] by free radical polymerization of *N*,*N*-dimethylacrylamide (DMAA) (18.33 g), methacryloyloxy benzophenone (MABP) (2.66 g), and sodium-4-styrenesulfonate (SSNa) (1.03 g) at a total monomer concentration of 200 mmol, using methanol as a solvent (100 mL) and α,α′-azobisisobutyronitrile (AIBN; 65.6 mg) as the initiator. After degassing the reaction mixture by four freeze–thaw cycles, the reactions were carried out at 60 °C for 20 hours under nitrogen. The polymer was purified by three precipitations in diethyl ether, typically yielding approximately 15.8 g (71.7%) of a white powder. The obtained molecular weight of the copolymer (M_w) was 335 kg mol^{-1} with a polydispersity index (PDI) of 2.8 and a MABP content of 5%. (Fig. 1).

As described previously by Weber *et al.*, Schönberg *et al.* and Alpsoy *et al.*[17,18,22] two syringes were filled with fluorinated oil (3M, Hamilton Bonaduz AG, Gastight Syringe, 500 L and Setonic GmbH, Glass Syringe, 1000 L-FC-3283) and linked to a syringe pump (Cetoni GmbH, NEMESYS 290N). The copolymer was first dissolved in deionized water (DI) water (110 mg mL^{-1}) by sonication and

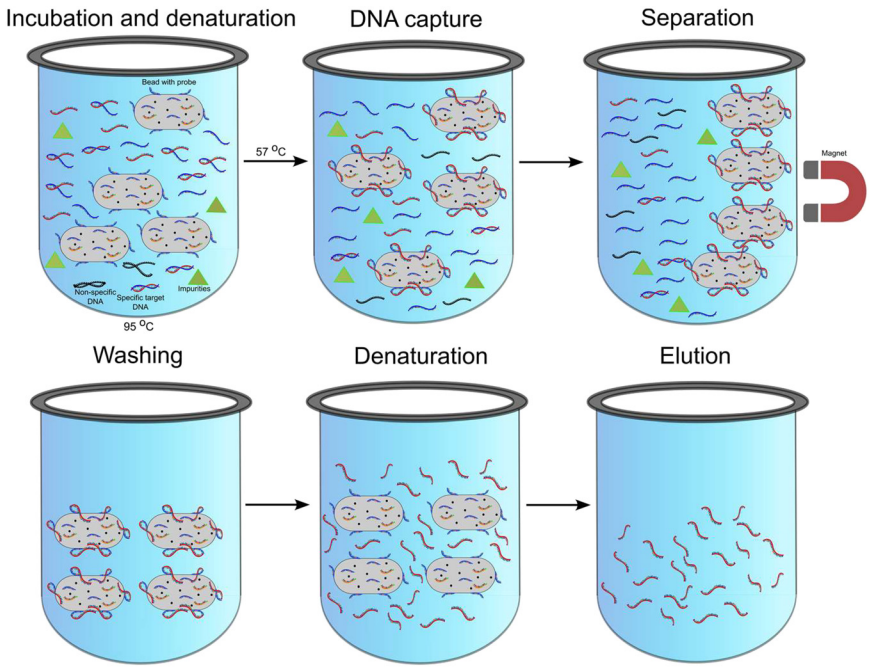

Fig. 1 Schematic of the workflow for DNA capture using hydrogel beads with probes (HBP) in a heterogeneous sample containing target DNA. Following the capture of the target DNA by the beads, magnetic separation is employed to isolate the DNA-bound beads from impurities. Subsequent washing steps are then conducted to further purify the captured DNA for downstream applications.

vortexing for 10–15 min. The polymer containing solutions were injected into a FEP tube (ProLiquid GmbH, Fluidflon FEP, ID: 0.25 mm) using a syringe pump. The tubes exiting the syringes were connected to a T-junction (VICI AG International, CTFE TEE connector), then coiled inside a UV chamber. The copolymer was cross-linked by exposure to 365 nm UV light at an irradiation intensity of 28 mW cm^{-2} for 15 minutes using a high-performance xenon lamp (Vilber GmbH), ensuring complete cross-linking.[18] Finally, the produced beads were collected in a 96-well microplate placed on a ThermoCell mixing block and washed with DI-water several times (Fig. 2).

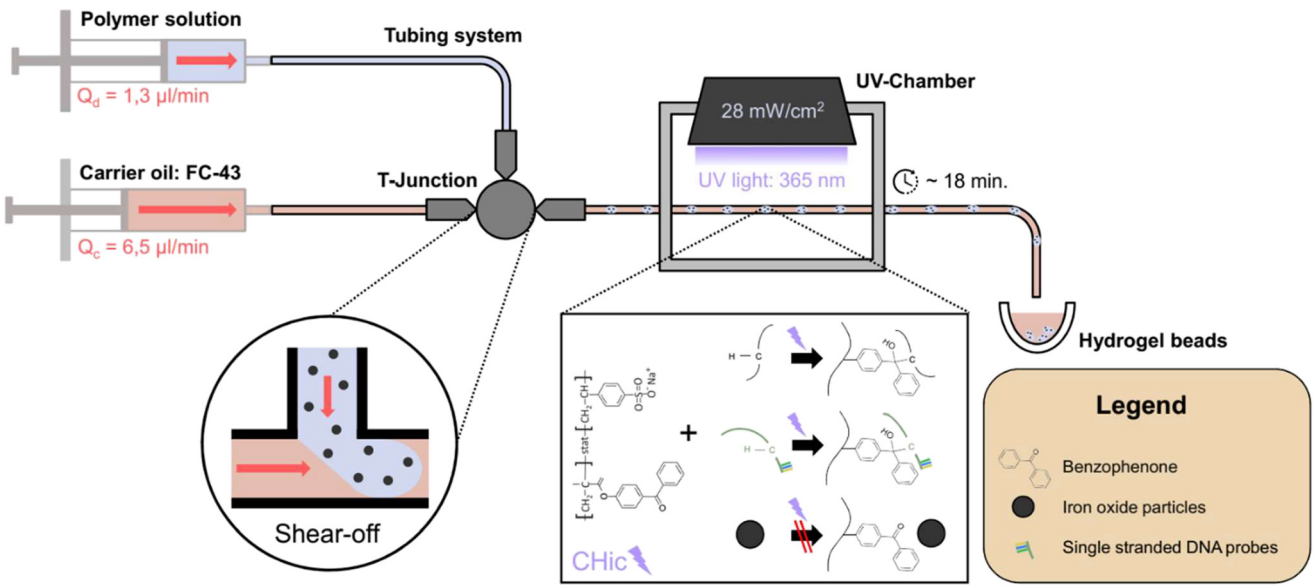

Fig. 2 Schematic depiction of the setup of the microfluidic system used to produce hydrogel beads. Shear-off of the dispersed phase, *i.e.* the polymer solution with added components, creates monodisperse plugs, which is then cross-linked in an UV chamber at a wavelength of λ = 365 for about 18 minutes. The insert shows the reaction scheme of a CHic reaction with benzophenone as a cross-linker, reproduced from Prucker *et al.*[23]

Production of hydrogel beads with oligo-Cy3, magnetic nanoparticles and probe

The polymer solution (110 mg mL^{-1}) was mixed with superparamagnetic Fe_3O_4 nanoparticles (Sigma, 1317-61-9, concentration 15 mg mL^{-1}), Cy3-labeled oligonucleotide (oligo-Cy3) at a concentration of 1.67 μM (5′-Cy3-TTTTTTTTT TTTTTT TT TCA AGA ACT ATG CTT CAA GCA GAC ATC, TIB MOLBIOL GmbH) and probe concentration of 16.67 μM (TTTTTTTTTTTTTTT TCT CGT GTA GAA ATT GCT TTG AGC, TIB MOLBIOL GmbH) (M_w = 11 936 g mol^{-1}). From these solutions, hydrogel beads comprising oligo-Cy3, a probe, and magnetic particles were manufactured using a flow rate ratio of 1 : 5 (Table 1 and Fig. 3). Using the advantages of CHic chemistry, the commercially synthesized probe specific to the target DNA was covalently immobilized onto the hydrogel beads. The porous structure and large internal surface area of the HBP enable the immobilization of a high number of probes, significantly enhancing the hybridization efficiency. The number of the probes was calculated to be 3.1×10^{11} per bead. Following the production of the beads, a three-stage PBS-Tween (0.1 wt%) wash was performed to remove residual oil. To characterize the beads, they were analyzed in a fluorescent reader (FLAIR™ reader, Sensovation, Radolfzell, Germany) at 50 ms in the green and red channels.

Characterization of the HBP by confocal fluorescence microscopy

To evaluate the distribution of probes in the beads, HBP were prepared and thoroughly washed. The fluorescence signal of the oligo-Cy3, used as a model to demonstrate probe distribution, was analysed with a confocal microscope. Additionally, the penetration depth of target DNA was determined by analyzing the fluorescence intensity of Cy5-labeled DNA following a one-hour incubation with the beads at 100 rpm. High-resolution Z-stack imaging was performed to capture fluorescence data across multiple optical sections spanning the entire bead volume. This technique enabled precise three-dimensional visualization of the probe distribution within the bead matrix and the penetration depth of target DNA, effectively minimizing out-of-focus fluorescence and enhancing image resolution.

Detection of target DNA as a function of the process conditions

The wells of a microtiter plate were filled with 10 beads each from the same production process. The buffer was removed with a pipette, and then 200 nM Cy-5 labelled target DNA 5′ Cy5-GCT CAA AGC AAT TTC TAC ACG AGA TCC TCT CTC TGA AAT CAC TGA GCA GGA GAA AGA TTT TCT ATG GAG TCA CAG GTA AGT GCT AAA ATG GA-3′ contained in the incubation medium was added to the wells in varying concentrations. The wells were sealed, covered with an aluminium foil lid, and put on a shaker for 1 h at 100 rpm. Then, with the help of a neodymium bar magnet that fits into the spaces between the wells, the magnetic beads were collected at the well walls, and the incubation medium was removed with an Eppendorf pipette (Fig. 4). The magnet was removed, and 100 μl of PBS was added to each well using the pipette. Slight taps on the plate could unstuck the beads from the walls, and afterwards, the microtiter plate was covered with the aluminium foil lid and placed on the shaker for 5 minutes at 100 rpm. Once the time had passed, the lid was removed, the bar magnet was reinserted, and the PBS was removed again. This process was carried out a total of three times. After these repetitions, 100 μl of PBS was added to each well to evaluate the beads in the fluorescence reader at 50 ms. After fluorescent measurement, the beads used for PCR application.

PCR and agarose gel electrophoresis

The mixtures for the polymerase chain reaction (PCR) were prepared in Eppendorf tubes, with 50 μL of each mixture containing nuclease-free water (22.5 μL), Hot Start PCR Master Mix (25 μL), forward primer (0.25 μL), reverse primer (0.25 μL), and ten beads from the samples. A total of 20 PCR cycles were performed. A positive control was used in the form of 2 μL of target DNA (1 pM). Subsequently, gel electrophoresis was performed to conclude the experiment. The gel was prepared by combining 1 g of agarose with 40 mL of TAE, followed by microwave heating for three minutes to facilitate agarose dissolution. Should the sample require reheating, this can be accomplished in a microwave oven for a few minutes. Due to the evaporation that occurred during the process, distilled water was employed to supplement the volume that had been lost. Then, 4 μL of GelRed was added to the dissolved agarose, which was then poured into a tray and allowed to harden for 45 minutes. A plastic comb was then placed into the gel in order to create the necessary wells. The gel was positioned within the gel electrophoresis tray and entirely submerged in TAE buffer. Subsequently, the PCR product was combined with a loading buffer and introduced into the wells of the gel. The lid was then secured, and the gel electrophoresis was conducted for a period of 45 minutes at a voltage of 60 V. Subsequently, the gel was positioned on

Table 1 List of the naming conventions of the hydrogel beads produced in this study and their respective components in the concentrations used throughout the whole study

Type//component	Copolymer [mg ml^{-1}]	Iron oxide [mg ml^{-1}]	Probe [μM]	Oligo-Cy3 [μM]
Beads with copolymer	110	—	—	—
Beads with copolymer and magnetic nanoparticles	110	15	—	—
HBP	110	15	16.67	1.67

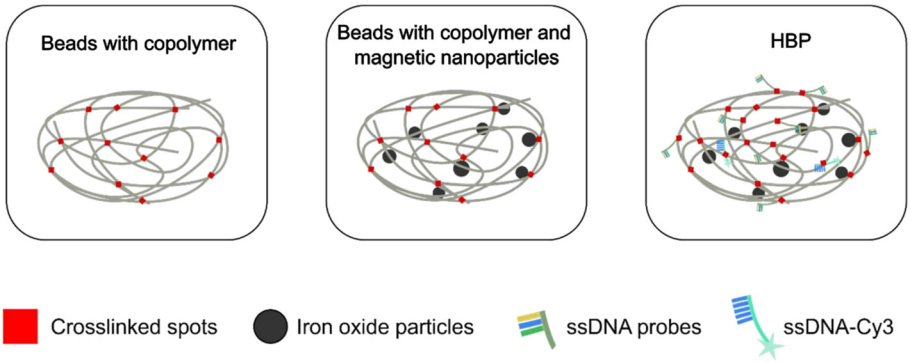

Fig. 3 Schematic depiction of the beads used in the study. The "beads with copolymer" were composed only of the copolymer and deionized water (DI-water). The "beads with copolymer and magnetic beads" are those that incorporate iron oxide particles into the copolymer without undergoing cross-linking. The third type, designated "HBP", in addition to the magnetic particles, contains two distinct single-stranded DNA (ssDNA) molecules. One ssDNA molecule serves as a probe for the selective capture of nucleic acids in a sample, while the other ssDNA is labelled with Cy3 to enhance bead visibility in the fluorescent reader.

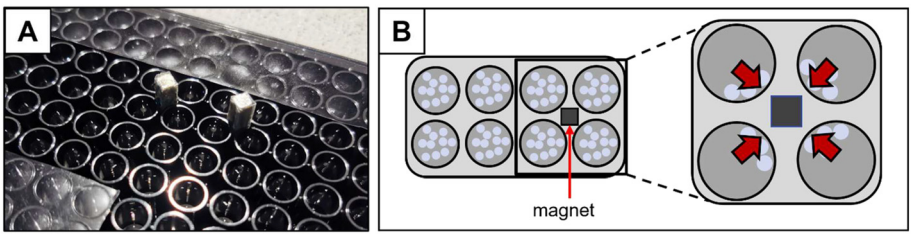

Fig. 4 A) Image of a microtiter plate during the washing step with the bar magnet in between the wells. The magnet will cause beads with integrated magnetic particles to clump together on the wall. B) A schematic depiction of the process.

a UV tray and transferred to the imaging system, where a snapshot was taken to ascertain the success of the PCR.

To capture the same sequence from native MCF-7 DNA by using HBP, MCF-7 DNA was extracted and purified using a commercially available kit and protocol (QIAamp DNA Mini Kit, 51304, Qiagen). The sequence from MCF-7 DNA was amplified using the same PCR protocol. The DNA concentrations were quantified using a commercial kit and protocol (Qubit dsDNA HS Assay, Q32851, Thermo Fisher Scientific). A solution containing 200 nM DNA was first incubated at 95 °C for 5 minutes, followed by cooling to 57 °C and incubating for 30 minutes at 300 rpm with ten beads present (Fig. 5). Afterwards, the beads were subjected to a washing process in accordance with the previously outlined methodology. Subsequently, the beads were employed in the polymerase chain reaction (PCR) and electrophoresis procedure, as illustrated in Fig. 5.

Determination of the probe accessibility

To calculate the probe accessibility in the HBP, a standard curve was prepared using fluorescently labelled target DNA at concentrations ranging from 0 to 50 nM, with fluorescence measurements recorded at an illumination time of 5 ms in the fluorescent reader. Subsequently, the beads were incubated with the 0–400 nM concentrations of fluorescently labelled DNA in PBS overnight at room temperature to ensure saturation. After incubation, the beads were washed three times with PBS-Tween (0.1 wt%) to remove unbound DNA. Fluorescence measurements were subsequently taken in the red channel with a readout time of 5 ms. Using the standard curve, the concentration of DNA captured by the beads was quantified, and the probe accessibility was calculated based on the known number of probe molecules per bead (3.1×10^{11} per bead).

Lower limit of detection quantification

To determine the lower detection limit, HBP beads were incubated with target DNA in serum at concentrations ranging from 0 to 2 nM while shaking at 100 rpm for 1 hour. Following incubation, the beads were washed three times with PBS-Tween (0.1 wt%) to remove unbound DNA. The washed beads were then used for the quantitative polymerase chain reaction (qPCR) analysis. qPCR was performed using the Capital qPCR Green Mix (4×) (biotechrabbit GmbH) according to the manufacturer's protocol. Each reaction was prepared in a final volume of 20 μL, consisting of 5 μL of the 4× Capital qPCR Green Mix, 0.25 μM forward primer, 0.25 μM reverse primer, and 2 μL of the respective template. For the experimental sample, 2 μL of bead suspension containing 10 beads with captured DNA was used. A positive control reaction included 2 μL of template DNA (1 pM), while a negative control reaction contained 2 μL of nuclease-free water to verify the absence of contamination in the reagents.

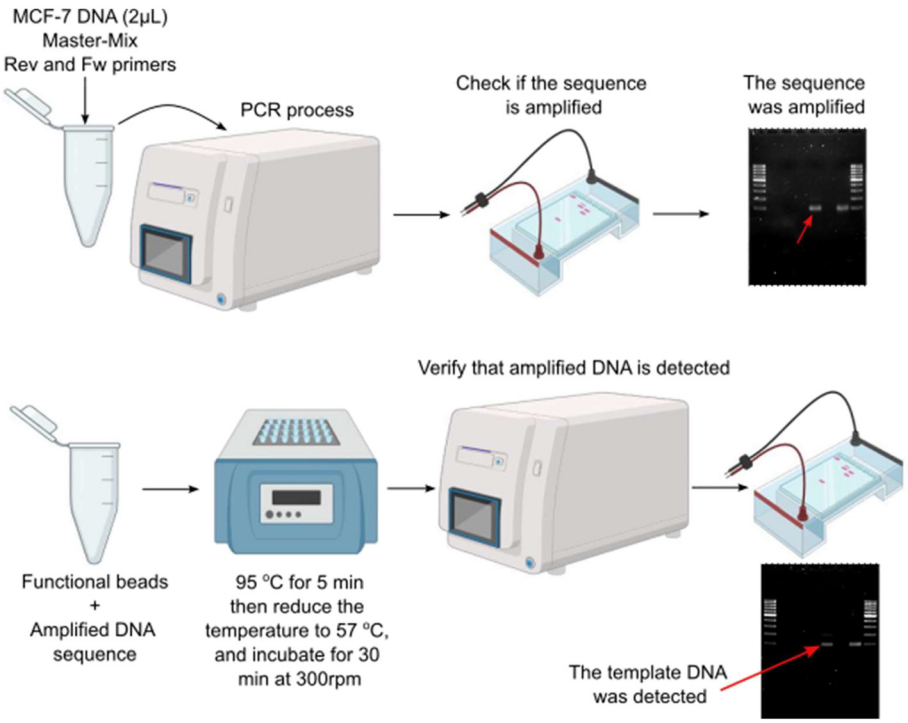

Fig. 5 MCF-7 DNA was isolated and amplified through PCR. Subsequently, the amplified DNA sequence, suspended in PBS, was incubated with the HBP. To denature the DNA sample, it was subjected to a thermal treatment at 95 °C for 5 minutes, followed by cooling to 57 °C and incubation for 30 minutes. Verification of DNA capture by the HBP was carried out using PCR analysis.

Additionally, a no-template control (NTC) was set up using nuclease-free water as the template to confirm the absence of non-specific amplification. The qPCR reactions were performed in a thermal cycler under the following conditions: an initial denaturation step at 95 °C for 2 minutes, followed by 25 cycles of denaturation at 95 °C for 15 seconds and annealing/extension at 60 °C for 30 seconds. Fluorescence signals were recorded during the annealing/extension step in each cycle, and the data were analysed to evaluate amplification efficiency and specificity.

Statistical analysis

All statistical analyses were performed using Welch's ANOVA, followed by the Bonferroni post-hoc test to assess differences between groups. The comparisons included (i) signal densities of target DNA in PBS, serum, and blood at different concentrations, (ii) signal densities of different concentrations of target DNA in undiluted blood and serum and (iii) probe accessibility. A p-value of less than 0.05 ($p < 0.05$) was considered as statistically significant. All analyses were performed using SPSS version 19.02.0(20).

Ethical statement

All experiments were performed in accordance with the Guidelines of Votum 309/15 and 309/16 and experiments were approved by the ethics committee at University Hospital Freiburg, Germany. Informed consents were obtained from human participants of this study.

3. Results and discussion

Production and characterization of the HBP

The functionalized beads were synthesized using a combination of droplet-based microfluidics and the CHic photochemistry as described previously.[17,18,22] During UV illumination the CHic process simultaneously cross-links the photopolymer confined in the droplet and attaches the (labelled) probes covalently to the forming network. After this they are washed and analysed using a fluorescence reader in the green channel. The size of the beads was determined from the fluorescence images using the ImageJ software. All beads were rather homogenous in size, with a coefficient of variation, calculated from 60 beads per type, below 5% (Fig. 6). Specifically, the CV values for beads with copolymer alone, beads with copolymer and magnetic particles, and HBP were 3.6%, 3.6%, and 4.4% for the length of beads and 3.5, 3.4 and 4.3% for the width of the beads, respectively. The beads containing the magnetic particles were 10% longer, probably due to a higher viscosity of the solutions during droplet generation. The size of the beads can be tuned by adjusting the concentration of the polymer, the extent of cross-linking (cross-linker contents, dose of irradiation), and the ratio of flow rates between the carrier and plug fluid.[17] Before starting with the assay development, the blank signal of the different hydrogel beads was measured in order to assess their impact on subsequent experiments. The mean signal density in the red channel was approximately 30% of that in the green channel for all three bead types, most likely

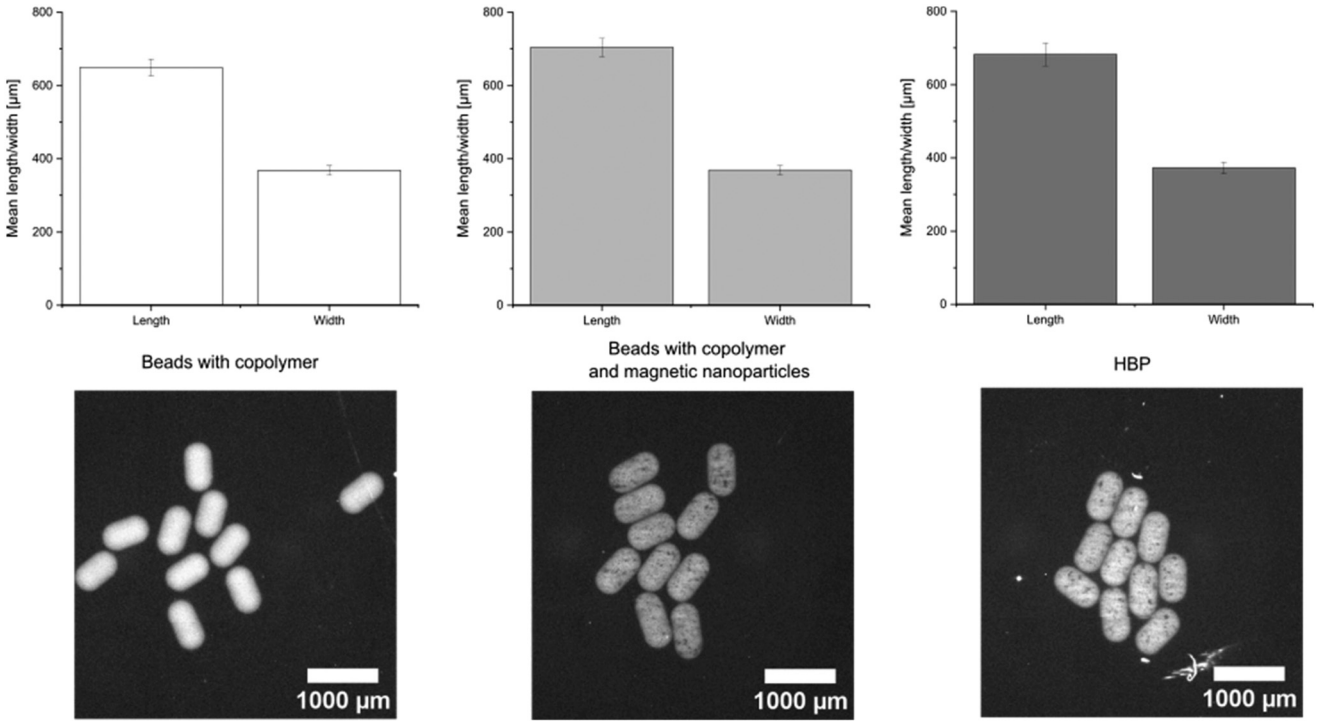

Fig. 6 Measurement of the length and width of polymer-only beads as well as the same with added, magnetic particles and completely the HBP together with the corresponding fluorescence images. Number of measured beads n was n = 60 beads per column. The images from the fluorescence reader are adjusted to display gray values from 100–4000.

due to light absorption and scattering by the integrated magnetic particles.[17,22] It should be noted, that the HBP exhibited a low blank signal in the green channel and an even lower signal in the red channel (Fig. 7).

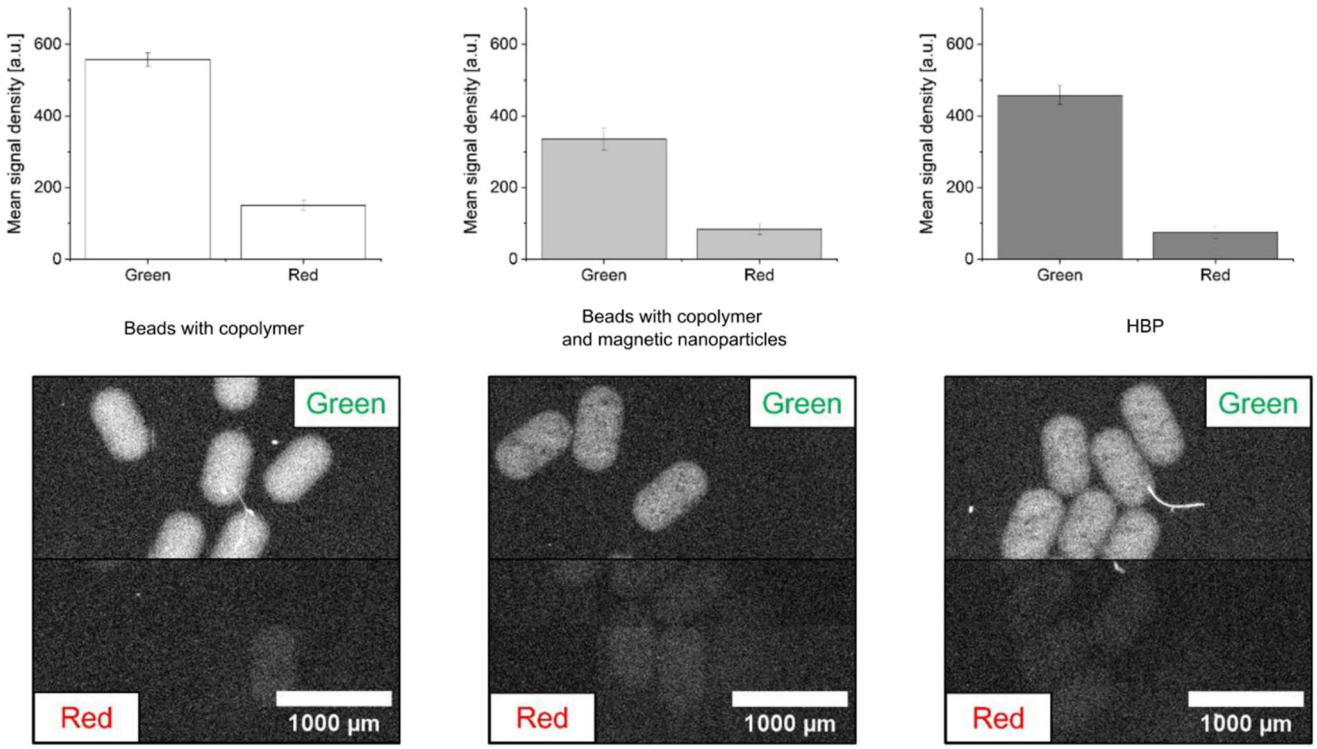

Fig. 7 Measured signal densities of the blank signal of the different bead types and their respective images in the green and red channels with an illumination time of 50 ms. The number of measured beads was 60 per column, and the displayed gray values range from 0–1000 for all images.

To assess the probe distribution in the beads, the beads with oligo-Cy3 were prepared and incubated with Cy5 labelled target DNA and then analysed using confocal microscopy. Z-stack images obtained using confocal microscopy revealed a homogeneous distribution of both Cy3 and Cy5 signals within the hydrogel beads. A slight shift in the signal maxima and reduced intensity at the bead edges were observed, likely due to the shape of the beads. Minor fluctuations in the Cy3 signal at the beginning of the scan may result from high-sensitivity imaging settings and background noise (Fig. 8).

Detection and quantification of the target DNA

To further analyze the binding of the target DNA in varying media and study any potential dilution effects, the HBP were incubated in 100 μl of the media at different concentrations (diluted with PBS), with a constant target DNA concentration of 200 nM. The media tested included PBS, human AB serum, and whole blood at concentrations of 100%, 50%, 25%, and 12.5%. Subsequently, after a one-hour incubation period and washing procedure, the signal densities of the beads were quantified in the red channel using a fluorescence reader with an illumination time of 50 milliseconds. The resulting images and the measured signal densities at the different concentrations are presented in Fig. 9. The signal densities remained constant within the different media and the different dilutions, indicating that the incubation medium had no significant impact on the process.

In the next experimental series, the binding efficiency was recorded at varying target DNA concentrations in pure serum and blood. The HBP were incubated in 100 μl of undiluted serum or blood containing target DNA at concentrations of 3.125 nM, 6.25 nM, 12.5 nM, 25 nM, 50 nM, 100 nM, and 200 nM. The incubation period was 60 minutes, during which time the samples were shaken at 100 rpm, followed by a washing step. As illustrated in Fig. 10, the graphs demonstrate an increase in signal density with rising target DNA concentrations spiked into both serum and blood. The low background signals show that there is no significant increase of the signal through non-specific interactions or binding with the surface of hydrogel beads.[24] The results obtained in this study are comparable to those reported in the literature regarding the concentration range of target DNA. However, our approach allows for a tenfold reduction in the required sample volume. While the literature typically utilizes approximately 1 mL of blood sample, this study achieves comparable results with a sample volume that is by a factor of ten smaller. This reduction in sample volume confines the reaction to a smaller space, which significantly

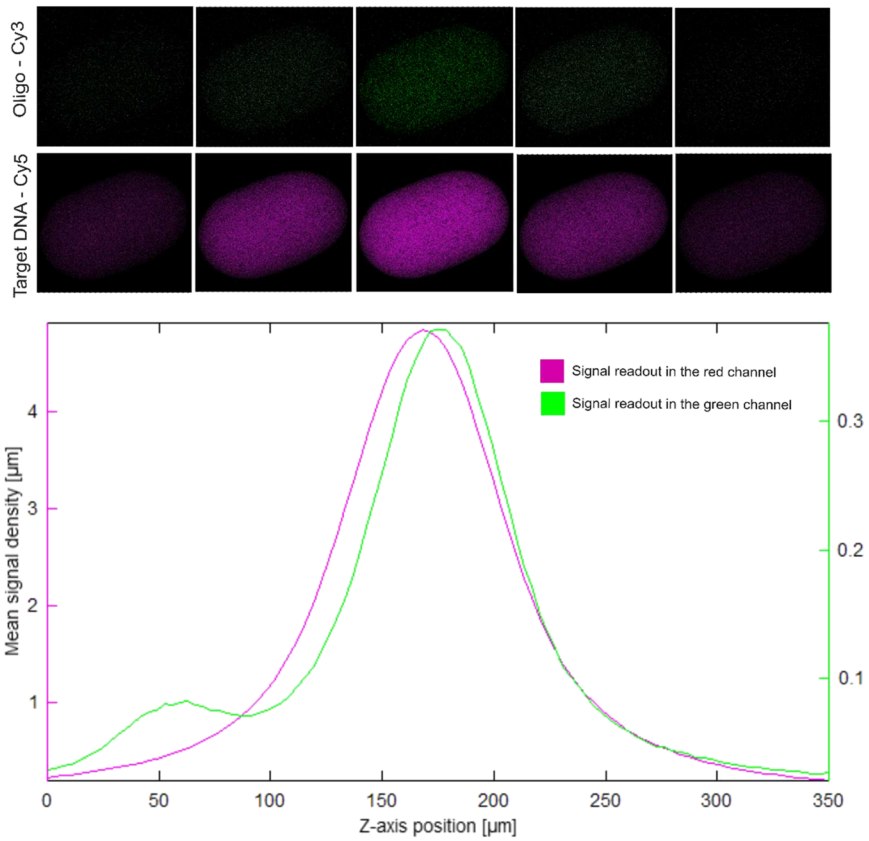

Fig. 8 Line plot of a Z-stack experiment of a functionalized bead incubated without target DNA in a confocal microscopy experiment. The measured signal is from the oligo-Cy3, which shows the probe distribution throughout the bead. The *z*-axis plot shows the mean signal density over the *z*-axis throughout the bead.

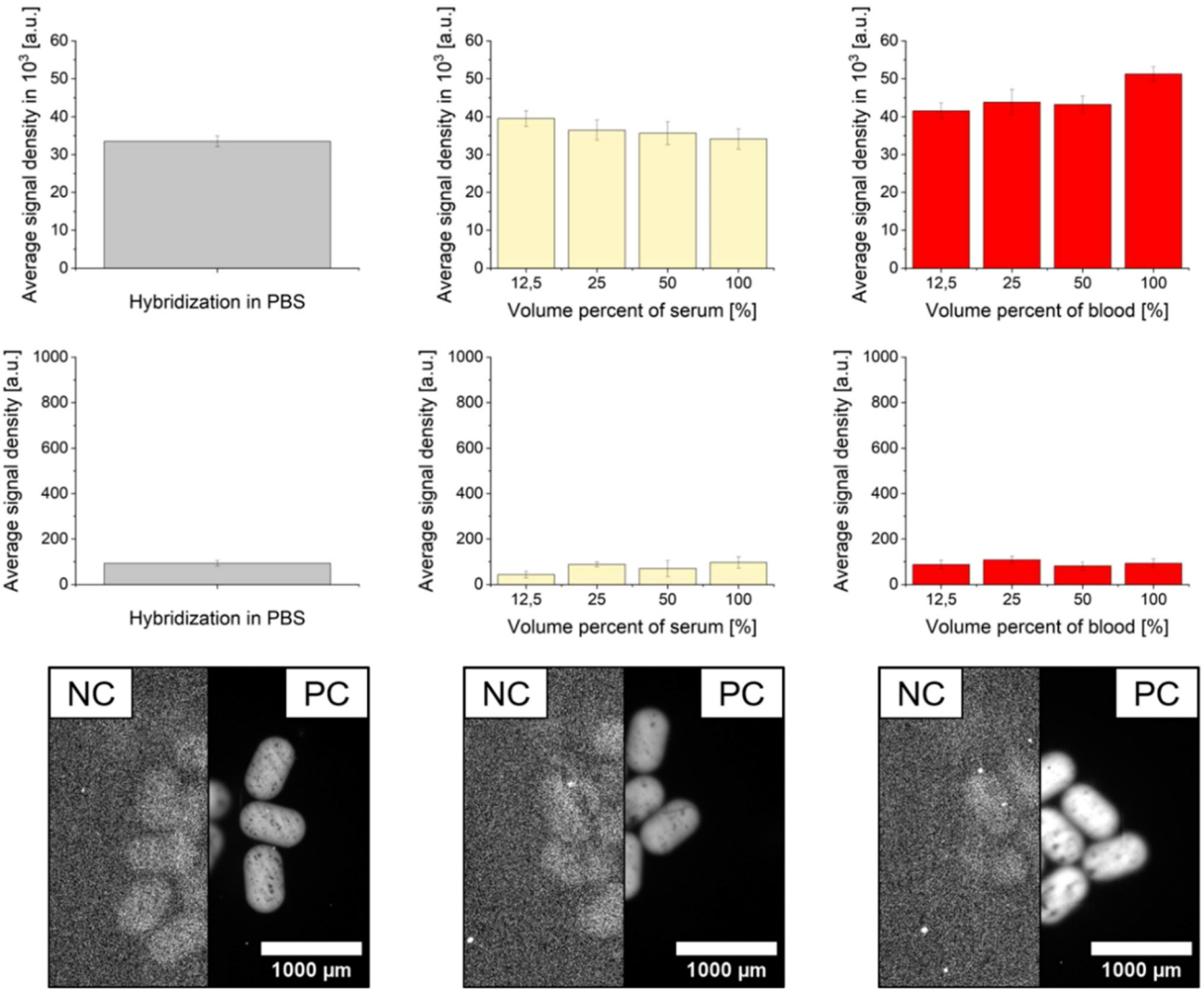

Fig. 9 Average measured signal densities for the beads incubated with the target DNA in PBS, serum, and blood in different concentrations. For each column, 10 beads were measured. The binding was tested twice for PBS, serum and blood, independently. The displayed gray values of the images are: NC: 0–500; PC: not changed. Error bars represent standard deviation of three independent experiments (n = 30). The difference between the dilutions of serum and blood was not statistically significant ($p > 0.05$).

enhances interaction efficiency and binding kinetics. As a result, the likelihood of specific interactions between the target DNA and hydrogel beads is notably increased.[14]

Amplification of target DNA captured by HBP in different media using PCR and electrophoresis

To check the potential of using the beads directly in downstream analysis, we washed the beads and placed them without any further treatment directly into a PCR reaction. To this the beads were incubated with or without the target DNA at a concentration of 200 nM in PBS, serum, and whole blood. Subsequently, the beads were thoroughly washed and ten beads were transferred directly into individual PCR tubes. The negative samples were prepared without the addition of labelled target DNA, while the positive samples were prepared with 200 nM of labelled target DNA. The positive control was performed using 1pM of target DNA. As illustrated in Fig. 11, DNA captured by HBP in the samples of PBS, serum, and blood was effectively amplified *via* PCR, and the presence of the amplified target DNA was confirmed by gel electrophoresis.

Detection of the target DNA in its natural state

Following the successful capture of DNA at 200 nM concentration for synthetic oligomers, an experiment was conducted to test the capture of the same sequence from real sample. For this purpose, genomic DNA was isolated from MCF-7 cells. Subsequently, the target sequence was amplified *via* PCR, and the DNA concentration of the PCR product was

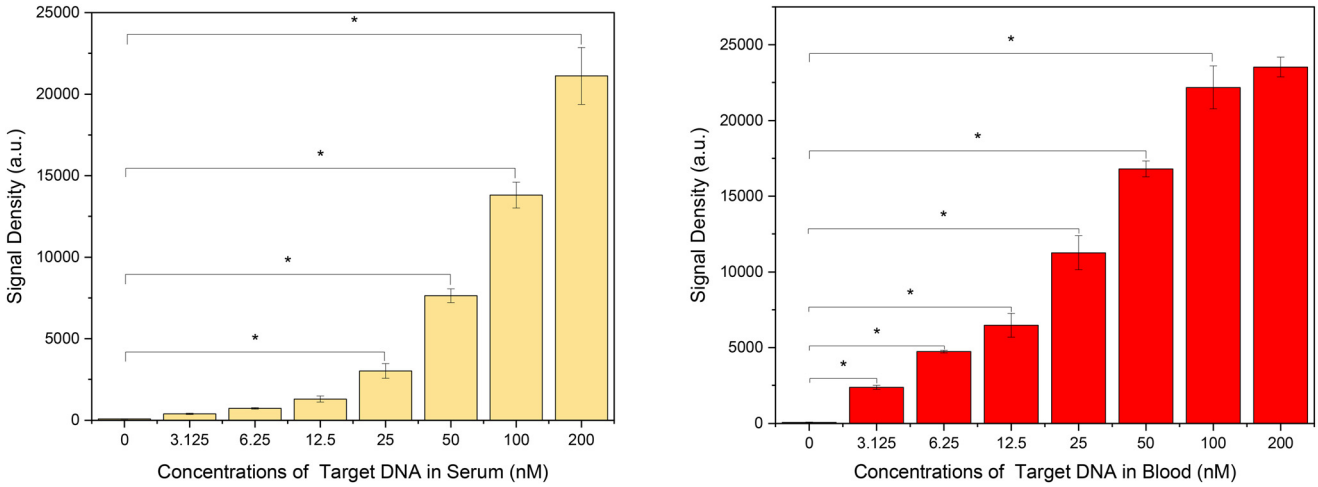

Fig. 10 Signal densities of beads incubated in undiluted serum or blood with different concentrations of added target DNA. The illumination time of the beads incubated in serum and blood was 50 ms. Error bars represent standard deviation of three independent experiments (n = 30) and blood was 50 ms. Error bars represent standard deviation of three independent experiments (n = 30). Differences between groups are indicated by an asterisk (*), indicating a statistically significant difference with a p-value <0.05. In the blood, no significant difference was observed between the 100 nM and 200 nM concentrations.

quantified using the ScanDrop spectrophotometer (Fig. 12a). The same concentration of the amplified sequence, in conjunction with the labelled target DNA, was employed in the subsequent capture experiment. The efficient detection of double-stranded DNA (dsDNA) was achieved by applying a thermal denaturation step, in which the DNA sample and HBP were heated to 95 °C for 5 minutes to generate ssDNA. This temperature, commonly used in standard PCR protocols to separate DNA strands, disrupts the hydrogen bonds between complementary strands, resulting in ssDNA that is available for hybridization with the immobilized capture probes. Immediately after denaturation, the temperature was reduced to 57 °C to allow specific hybridization between the target DNA and the bead-bound capture probes. The hybridization temperature of 57 °C was selected based on gradient PCR analysis as the optimal annealing temperature for specific primer–DNA binding (see ESI†). The HBPs used in our study exhibit thermal stability under these conditions, with no melting or structural degradation observed during incubation at 95 °C.[25] Following the washing steps, 10 beads were transferred into individual PCR tubes for amplification, and electrophoresis was conducted. As illustrated in Fig. 12b, the hydrogel beads were observed to effectively capture the DNA, thereby demonstrating their capability for target DNA capture from natural sources.

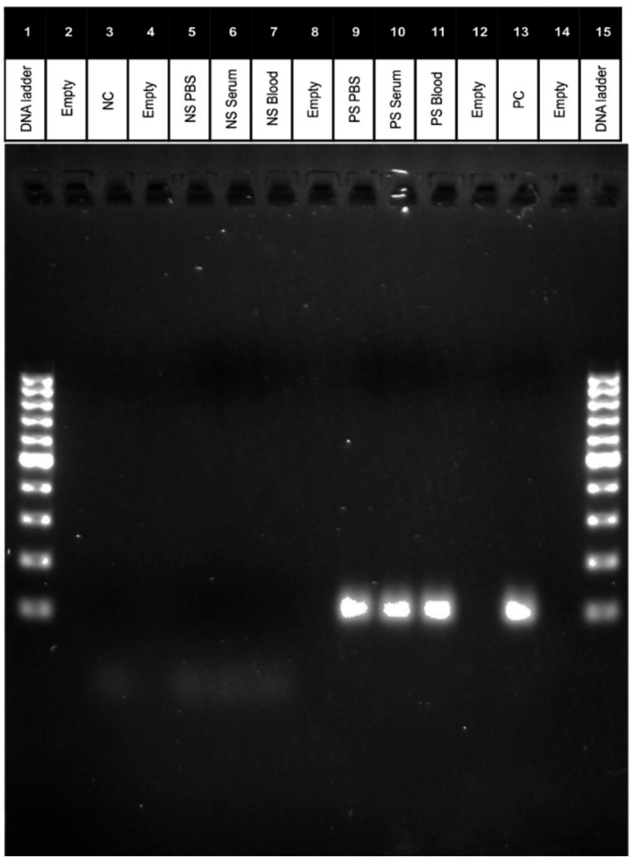

Fig. 11 DNA captured by HBP in PBS, serum, and blood samples was amplified using PCR and visualized on a gel. PS represents samples containing target DNA, while NS refers to negative controls without target DNA.

Determination of the probe accessibility

Determining probe accessibility is crucial for understanding binding efficiency, optimizing surface functionalization, and enhancing the sensitivity of the test platform.[14] To determine the probe accessibility of the hydrogel beads, a calibration curve was established using target DNA concentrations ranging from 0 to 50 nM, which served as a reference for the subsequent quantification (Fig. 13a). After incubating the HBP in a solution containing target DNA overnight and performing thorough washing with PBS to remove unbound

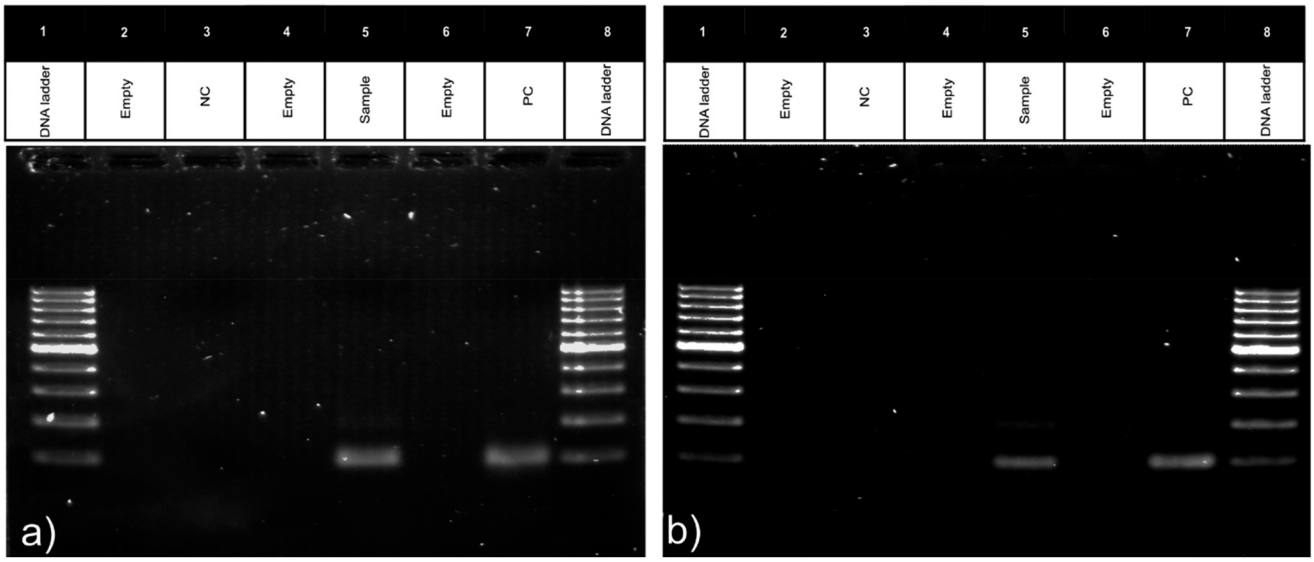

Fig. 12 Following the isolation of MCF-7 DNA, the target DNA sequence was amplified using PCR, resulting in the amplification of a 92-base pair (bp) DNA sequence (a). The amplified MCF-7 DNA sequence was captured by the HBP and subsequently verified through PCR analysis (b).

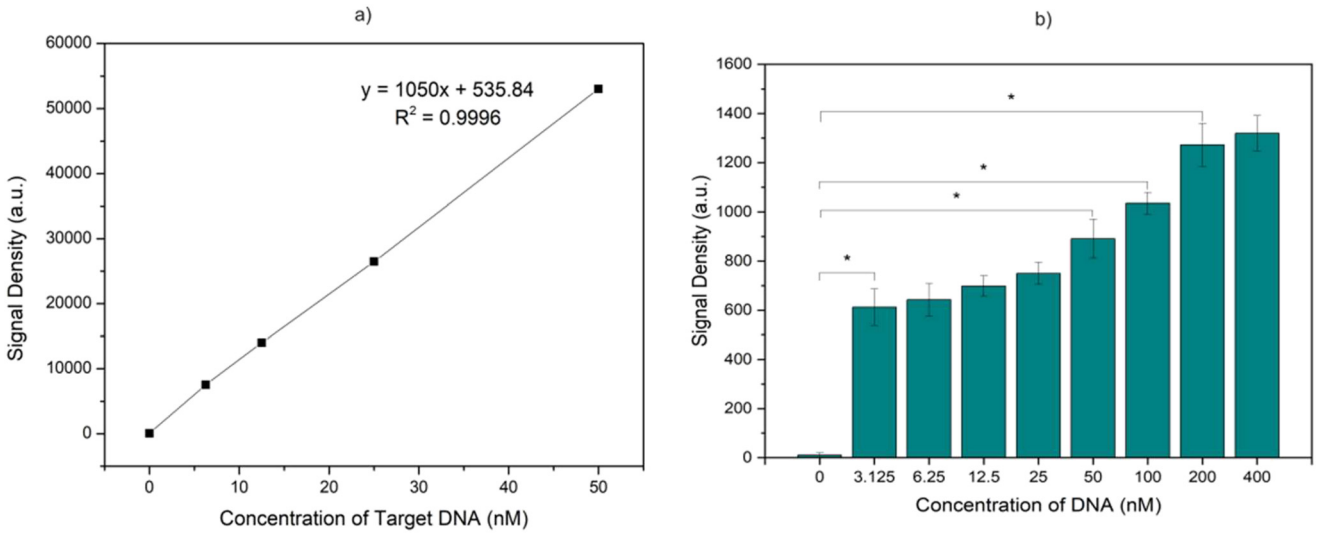

Fig. 13 Calibration curve between DNA concentration and signal density (a). Signal densities of DNA captured by beads at varying concentrations (signal integration 5 ms) (n = 3) (b). Differences between groups are indicated by an asterisk (*), indicating a statistically significant difference with a p-value <0.05. No significant difference was observed between the 200 nM and 400 nM concentrations, as well as among the 3.125 nM, 6.25 nM, 12.5 nM, and 25 nM concentrations.

DNA, the signal density for each bead group was measured. The constant signal density observed in the two highest concentration groups are most probably due to saturation of the beads with target DNA (Fig. 13b). The difference between the 200 and 400 nM concentrations was not statistically significant ($p > 0.05$).

Saturation of the beads with target DNA was achieved at concentrations above 200 nM, where the average signal density of the beads was measured as roughly 1300 a.u. (arbitary units). Using this signal density and the slope of the standard curve, the number of target DNA molecules captured per bead was calculated to be 4.2×10^{10}. Based on the known number of probe molecules on the beads (3.1×10^{11} molecules per bead), the probe accessibility was determined to be 13%, demonstrating a high level of target DNA capture efficiency (Fig. 13).

Quantification of the lower limit of detection

After determining the DNA capture efficiency at a concentration of 200 nM, the ability of the HBP to capture target DNA at lower concentrations was evaluated. For this purpose, varying concentrations of target DNA ranging from 0.0125 nM to 2 nM in 100 μL serum were incubated with the HBP. Following incubation, the beads were washed three times with PBS-Tween (0.1 wt%), and

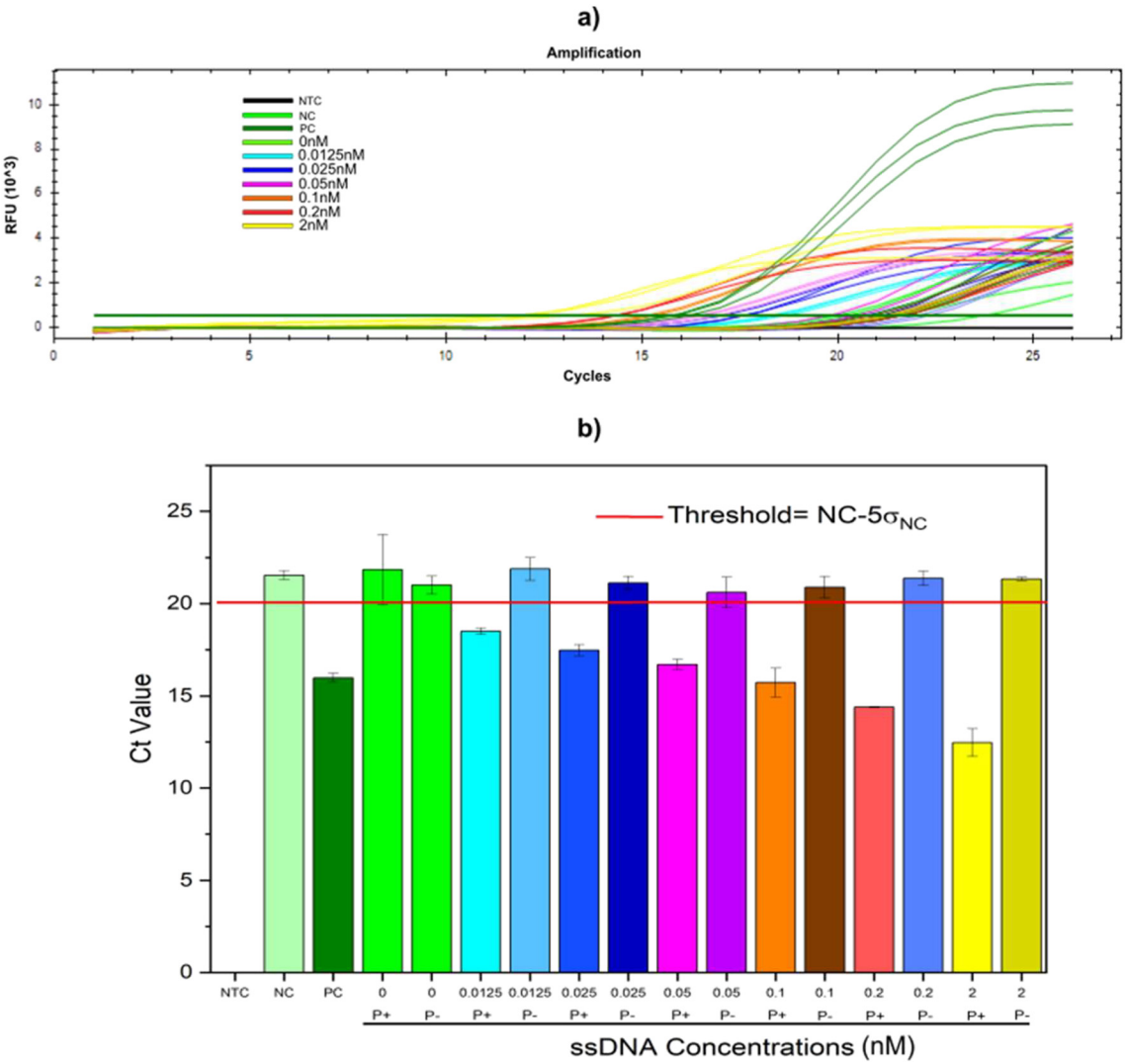

Fig. 14 Assessment of target DNA capture efficiency by the HBP across various concentrations (ranging from 0 to 2 nM) in serum. Following incubation and subsequent washing steps, DNA captured by the beads was used for qPCR (a) amplification curves b) CT values of the experiments shown in a); solid line gives the threshold defined as value of the negative control minus 5 times the standard deviation. The legends for amplification curves of hydrogel beads without probe are not shown, as their signals closely resemble those of the NC group. Error bars represent the standard deviation of three independent experiments (n = 3). NC: negative control, NTC: no template control, PC: positive control. P+: HBP, P−: hydrogel beads without probe.

used for the qPCR procedure. Fig. 14 presents amplification data for a PCR assay, showing fluorescence intensity (RFU) *versus* cycle number in panel (a) and corresponding Ct values in panel (b). The results demonstrate strong assay specificity and sensitivity: no amplification was observed in the negative controls (NTC and NC), while the positive control (PC) exhibited early amplification. As expected, amplification efficiency increased with higher DNA concentrations, as indicated by earlier Ct values for higher concentrations (0.0125 to 2). The limit of detection (LOD) in serum, calculated from blank measurements, was determined to be 0.36 ng mL^{-1} (0.0125 nM). The LOD was defined as the signal corresponding to the mean of the negative control (NC) minus five times the standard deviation (LOD = NC_{mean} − $5\sigma_{NC}$), based on the negative slope observed in the PCR amplification curve. Although the standard approach typically uses 3.3 × σ_{NC} (ref. 14) we opted for a more stringent criterion by employing 5 × σ_{NC} to ensure high confidence in our results. Despite this conservative threshold, our data consistently demonstrate a clear distinction between the target signals and the negative control even at a concentration of 0, underscoring the sensitivity and reliability of our method. The lower maximum RFU values observed in the bead-containing samples compared to the positive control are attributed to the presence of hydrogel beads in the PCR mixture. These beads can partially interfere with the binding efficiency of the fluorescent dye to the amplified DNA, resulting in slightly reduced fluorescence signal intensity.

Our cfDNA detection method demonstrated a detection limit of 0.36 ng mL^{-1}, making it more sensitive than commercially available cfDNA detection kits.[11–13] For example, Jiang *et al.* (2020) reported a detection limit of 5.57 ng mL^{-1},[26] while Zhong (2022) and Raymond (2020) achieved 4.34 ng mL^{-1} from plasma in samples having mL volumes.[11,13] It is interesting to compare these values to concentrations typically observed in cancer diagnostics. The median concentration of circulating cfDNA varies among different cancer types, with measured values ranging from 2 ng mL^{-1} in melanoma to 53 ng mL^{-1} in castration-resistant prostate cancer. In general, cfDNA levels are higher in breast and prostate cancers, with ranges spanning from 0.5 to 1600 ng mL^{-1} in breast cancer and 7 to 1177 ng mL^{-1} in castration-resistant prostate cancer.[14] Thus the sensitivity of our bead assay is well within the critical clinical range.

Another advantage of the system described here is the low sample volume requirement of only 100 μL, compared to the 0.24–10 mL typically required by commercial kits.[14] This makes it ideal for applications involving valuable clinical or research specimens, as the requirements for rare or limited samples are significantly reduced. In addition, the low-volume design minimizes reagent consumption, improving cost-effectiveness and scalability for high-throughput applications.

4. Conclusion

The analysis of cfDNA and ctDNA from complex biological samples such as blood or urine is a promising way to advance cancer diagnostics. However, the current methods for capturing cfDNA face a number of challenges, including the immobilization of probes on surfaces, the reduction of non-specific binding, low sensitivity and recovery yields, the inefficient capture of short DNA fragments, and high cost. The present study introduces a hydrogel bead platform that effectively addresses these issues. An attractive feature of the developed process is that the synthesis of these hydrogel beads is achieved in a single reaction step through a combination of droplet-based microfluidics and photo-induced C, H insertion cross-linking reactions, which allows for easy incorporation of magnetic particles and probe immobilization. The integration of probes and optimization of surface chemistry leads to a notable enhancement in the sensitivity and yield of cfDNA extraction from serum and blood samples. The cfDNA detection limit of 0.36 ng mL^{-1} concentration represents one of the most sensitive and efficient cfDNA detection techniques reported to date.

The hydrogel beads with bound DNA can be used directly in downstream PCR processes, eliminating the risk of DNA loss or contamination commonly associated with conventional elution techniques. This has the potential to improve the recovery and purity of cfDNA, thereby improving the overall performance of cfDNA analysis in various sample types. As an example, the DNA mutation (c.1633G>A:E545K) in MCF-7 cells was successfully captured from both serum and whole blood using the developed hydrogel beads. Identification of the c.1633G>A (E545K) mutation in the PIK3CA gene is critical for understanding tumor biology because it activates the PI3K/AKT pathway, which drives cancer cell growth and survival. It also helps to personalize treatment by identifying patients who may benefit from targeted therapies and provides insight into disease prognosis and potential new drug development.

In conclusion, the application of magnetic hydrogel beads functionalized with immobilized probes represents a promising approach to advance cfDNA analysis, which has the potential to make significant contributions to biomedical research and clinical diagnostics.

Data availability

The raw data supporting the findings of this study are available in the e-lab repository at the Laboratory for Process Technology, University of Freiburg. The dataset can be accessed at **https://svn.cpi.imtek.uni-freiburg.de**. Access may require registration or specific permissions.

Conflicts of interest

The authors declare no competing financial interest.

Acknowledgements

We thank the DFG (Project number: RU489/31-2, TH1358/3-2) and the German Federal Ministry for Economic Affairs and Climate Action project number KK5033111 for their financial support.

References

1 W. Wang, Y. He, F. Yang and K. Chen, Current and emerging applications of liquid biopsy in pan-cancer, *Transl. Oncol.*, 2023, **34**, 101720.
2 J. Noor, A. Chaudhry, R. Noor and S. Batool, Advancements and Applications of Liquid Biopsies in Oncology: A Narrative Review, *Cureus*, 2023, **15**, e42731.
3 M. Ilié and P. Hofman, Pros: Can tissue biopsy be replaced by liquid biopsy?, *Transl. Lung Cancer Res.*, 2016, **5**, 420–423.
4 M. Nikanjam, S. Kato and R. Kurzrock, Liquid biopsy: current technology and clinical applications, *J. Hematol. Oncol.*, 2022, **15**, 131.
5 R. J. Diefenbach, J. H. Lee, R. F. Kefford and H. Rizos, Evaluation of commercial kits for purification of circulating free DNA, *Cancer Genet.*, 2018, **228–229**, 21–27.
6 Y. Hu, D. Chen, J. V. Napoleon, M. Srinivasarao, S. Singhal, C. A. Savran and P. S. Low, Efficient capture of circulating tumor cells with low molecular weight folate receptor-specific ligands, *Sci. Rep.*, 2022, **12**, 8555.
7 S. N. Lone, S. Nisar, T. Masoodi, M. Singh, A. Rizwan, S. Hashem, W. El-Rifai, D. Bedognetti, S. K. Batra, M. Haris, A. A. Bhat and M. A. Macha, Liquid biopsy: a step closer to

transform diagnosis, prognosis and future of cancer treatments, *Mol. Cancer*, 2022, **21**, 79.

8 S.-C. Liu, Circulating tumor DNA in liquid biopsy: Current diagnostic limitation, *World J. Gastroenterol.*, 2024, **30**, 2175–2178.

9 G. Siravegna, S. Marsoni, S. Siena and A. Bardelli, Integrating liquid biopsies into the management of cancer, *Nat. Rev. Clin. Oncol.*, 2017, **14**, 531–548.

10 B. N. Hapsianto, N. Kojima, R. Kurita, H. Yamagata, H. Fujita, T. Fujii and S. H. Kim, Direct Capture and Amplification of Small Fragmented DNAs Using Nitrogen-Mustard-Coated Microbeads, *Anal. Chem.*, 2022, **94**, 7594–7600.

11 H. Zhong, L. Zeng, M. Tao, Y. Ye, Y. Wang, L. Hou, M. Wu, H. Liu, H. Zhang and M. Tang, A novel method for extracting circulating cell-free DNA from whole blood samples and its utility in the non-invasive prenatal test, *Prenatal Diagn.*, 2022, **42**, 1173–1181.

12 F. Janku, H. J. Huang, D. Y. Pereira, M. Kobayashi, C. H. Chiu, S. G. Call, K. T. Woodbury, F. Chao, D. R. Marshak and R. Y. T. Chiu, A novel method for liquid-phase extraction of cell-free DNA for detection of circulating tumor DNA, *Sci. Rep.*, 2021, **11**, 19653.

13 C. K. Raymond, F. C. Raymond and K. Hill, UltraPrep is a scalable, cost-effective, bead-based method for purifying cell-free DNA, *PLoS One*, 2020, **15**, e0231854.

14 E. Polatoglou, Z. Mayer, V. Ungerer, A. J. Bronkhorst and S. Holdenrieder, Isolation and Quantification of Plasma Cell-Free DNA Using Different Manual and Automated Methods, *Diagnostics*, 2022, **12**, DOI: **10.3390/diagnostics12102550**.

15 Y. J. Kim, Y.-H. Cho, J. Min and S.-W. Han, Circulating Tumor Marker Isolation with the Chemically Stable and Instantly Degradable (CSID) Hydrogel ImmunoSpheres, *Anal. Chem.*, 2021, **93**, 1100–1109.

16 A. Roberts, D. Shahdeo and S. Gandhi, in *Immobilization Strategies : Biomedical, Bioengineering and Environmental Applications*, ed. A. Tripathi and J. S. Melo, Springer Singapore, Singapore, 2021, pp. 475–507.

17 L. Alpsoy, A. S. Sedeky, U. Rehbein, K. Thedieck, T. Brandstetter and J. Rühe, Particle ID: A Multiplexed Hydrogel Bead Platform for Biomedical Applications, *ACS Appl. Mater. Interfaces*, 2023, **15**, 55346–55357.

18 J.-N. Schönberg, M. Zinggeler, P. Fosso, T. Brandstetter and J. Rühe, One-Step Photochemical Generation of Biofunctionalized Hydrogel Particles via Two-Phase Flow, *ACS Appl. Mater. Interfaces*, 2018, **10**, 39411–39416.

19 B. A. Otieno, C. E. Krause and J. F. Rusling, Bioconjugation of Antibodies and Enzyme Labels onto Magnetic Beads, *Methods Enzymol.*, 2016, **571**, 135–150.

20 W. Li, L. Zhang, X. Ge, B. Xu, W. Zhang, L. Qu, C.-H. Choi, J. Xu, A. Zhang, H. Lee and D. A. Weitz, Microfluidic fabrication of microparticles for biomedical applications, *Chem. Soc. Rev.*, 2018, **47**, 5646–5683.

21 M. Rendl, A. Bönisch, A. Mader, K. Schuh, O. Prucker, T. Brandstetter and J. Rühe, Simple one-step process for immobilization of biomolecules on polymer substrates based on surface-attached polymer networks, *Langmuir*, 2011, **27**, 6116–6123.

22 T. A. Weber, L. Metzler, P. L. Fosso Tene, T. Brandstetter and J. Rühe, Single-Color Barcoding for Multiplexed Hydrogel Bead-Based Immunoassays, *ACS Appl. Mater. Interfaces*, 2022, **14**, 25147–25154.

23 O. Prucker, T. Brandstetter and J. Rühe, Surface-attached hydrogel coatings via C,H-insertion crosslinking for biomedical and bioanalytical applications (Review), *Biointerphases*, 2017, **13**, 10801.

24 P. E. Scopelliti, A. Borgonovo, M. Indrieri, L. Giorgetti, G. Bongiorno, R. Carbone, A. Podestà and P. Milani, The Effect of Surface Nanometre-Scale Morphology on Protein Adsorption, *PLoS One*, 2010, **5**, e11862.

25 F. D. Scherag, T. Brandstetter and J. Rühe, Raising the shields: PCR in the presence of metallic surfaces protected by tailor-made coatings, *Colloids Surf., B*, 2014, **122**, 576–582.

26 J. Jiang, S. Ye, Y. Xu, L. Chang, X. Hu, G. Ru, Y. Guo, X. Yi, L. Yang and D. Huang, Circulating Tumor DNA as a Potential Marker to Detect Minimal Residual Disease and Predict Recurrence in Pancreatic Cancer, *Front. Oncol.*, 2020, **10**, 528008.